



LAWRENCE  
LIVERMORE  
NATIONAL  
LABORATORY

# Two-Phase Emission Detector for Measuring Coherent Neutrino-Nucleus Scattering

*C. A. Hagmann and A. Bernstein*

**Dec 1, 2003**

IEEE Nuclear Science Symposium  
Portland, OR  
Oct 19-25, 2003

Approved for public release; further dissemination unlimited

This document was prepared as an account of work sponsored by an agency of the United States Government. Neither the United States Government nor the University of California nor any of their employees, makes any warranty, express or implied, or assumes any legal liability or responsibility for the accuracy, completeness, or usefulness of any information, apparatus, product, or process disclosed, or represents that its use would not infringe privately owned rights. Reference herein to any specific commercial product, process, or service by trade name, trademark, manufacturer, or otherwise, does not necessarily constitute or imply its endorsement, recommendation, or favoring by the United States Government or the University of California. The views and opinions of authors expressed herein do not necessarily state or reflect those of the United States Government or the University of California, and shall not be used for advertising or product endorsement purposes.

**Abstract**—Coherent scattering is a flavor-blind, high-rate, as yet undetected neutrino interaction predicted by the Standard Model. We propose to use a compact (kg-scale), two-phase (liquid-gas) argon ionization detector to measure coherent neutrino scattering off nuclei. In our approach, neutrino-induced nuclear recoils in the liquid produce a weak ionization signal, which is transported into a gas under the influence of an electric field, amplified via electroluminescence, and detected by phototubes or avalanche diodes. This paper describes the features of the detector, and estimates signal and background rates for a reactor neutrino source. Relatively compact detectors of this type, capable of detecting coherent scattering, offer a new approach to flavor-blind detection of man-made and astronomical neutrinos, and may allow development of compact neutrino detectors capable of non-intrusive real-time monitoring of fissile material in reactors.

## I. INTRODUCTION

Coherent neutrino-nucleus scattering is a famous but as yet untested prediction of the Standard Model [1]. The process is mediated by neutral currents (NC), and hence is flavor-blind. Despite having relatively high rates, neutrino-nucleus scattering is difficult to observe because its only signature is a small nuclear recoil of energy  $\sim$  keV (for MeV neutrinos), requiring a low detector threshold. Over the past two decades, a number of authors have suggested low-temperature calorimeters [1,2], gas detectors [3], and germanium ionization detectors [4] for measuring neutrino-nucleus scattering. In this paper, we study a two-phase (gas-liquid) ionization detector, which combines low energy threshold with large event rates.

Coherent neutrino-nucleus scattering has the cross section [1]  $\sigma \sim 0.4 \times 10^{-44} N^2 E^2 \text{ cm}^2$ , where  $N$  is the neutron number, and  $E$  is the neutrino energy in MeV. This formula is valid for neutrino energies up to about 50 MeV, and thus applies to reactor, solar, and supernova neutrinos. For a fixed neutrino energy, the recoil spectrum is linearly falling with an average energy  $\langle E_r \rangle = 1/3 E_r^{\text{max}} = 716 \text{ eV}$  ( $E^2/A$ ), where  $A$  is the atomic number of the target nucleus.

It is well known however, that recoiling atoms are less effective in producing secondary ionization or scintillation than electrons of the same energy. The ratio of the ionization (or scintillation) yield from atomic projectiles to that from electrons, referred to as the quench factor  $Q$ , generally decreases with energy and is material dependent. For example, measured  $Q$  factors in silicon [5] decrease from 0.41 to 0.26, for recoil energies of 21 keV and 3.3 keV respectively. An even smaller quench factor of  $Q = 0.15$  was reported for germanium [6], at a recoil energy  $E_r = 254 \text{ eV}$ .

C. Hagmann is with Lawrence Livermore National Laboratory, Livermore, CA 94550 USA (telephone: 925-423-6484, e-mail: hagmann1@llnl.gov).

A. Bernstein is with Lawrence Livermore National Laboratory, Livermore, CA 94550 USA (telephone: 925-422-5918, e-mail: bernstein3@llnl.gov).

A signal consisting of only a few electrons or photons is below threshold for conventional solid or liquid state detectors without internal amplification. Hence we propose a two-phase (gas-liquid) argon emission detector with an electroluminescence gap in the gas to provide gain. This scheme combines a large target density in the liquid with the capability of sensing single electrons. Its moderate cost and scalability, as compared to calorimetric detectors, make this technology a promising approach to NC based detection of reactor and astronomical neutrinos.

## II. RECOIL RATE AND IONIZATION YIELD

An attractive attribute of neutrino coherent scattering is its relatively large cross section compared to inverse beta decay. For reactor neutrinos ( $\Phi \sim 6 \times 10^{12} \text{ cm}^{-2} \text{ s}^{-1}$  at  $\sim 25 \text{ m}$  from a 3 GigaWatt thermal (GWt) core), the expected event rates before detection efficiencies are  $56 \text{ kg}^{-1} \text{ day}^{-1}$  for coherent scattering off argon, compared to  $2.8 \text{ kg}^{-1} \text{ day}^{-1}$  for the inverse beta decay reaction in  $(\text{CH})_n$ . Here we assumed a typical fuel mix of 61.9 %  $^{235}\text{U}$ , 6.7 %  $^{238}\text{U}$ , 27.2 %  $^{239}\text{Pu}$ , and 4.2 %  $^{241}\text{Pu}$ , with neutrino spectra and mix parameters taken from [7,8]. Figure 1 shows the expected argon recoil spectra of the dominant fissionable isotopes  $^{235}\text{U}$  and  $^{239}\text{Pu}$ . Although the average recoil energy is  $\sim 200 \text{ eV}$ , the majority of the recoil events do not produce primary ionization or excitation because of quenching.

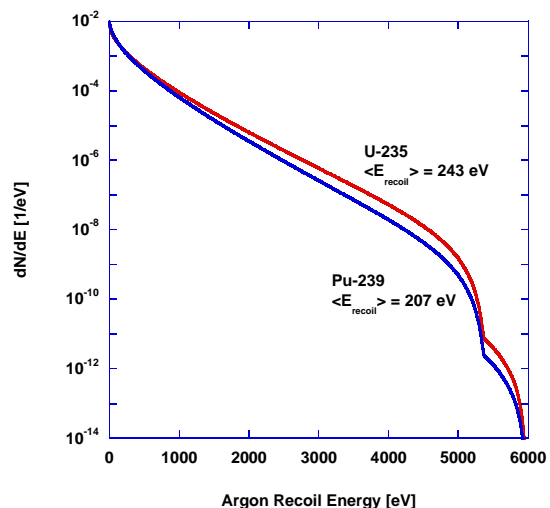


Fig. 1: Nuclear recoil spectra predicted for fission neutrinos scattering coherently off natural argon. The spectra are sensitive to the reactor fuel isotopics.

In order to estimate the amount of ionization produced by recoils, we performed a Monte Carlo simulation of the atomic collision cascade. Our computer calculations are based on the TRIM code [9], which models the collisions as a series of binary events separated by a path length  $L = n^{-1/3}$  ( $= 3.6 \times 10^{-8}$  cm in liquid argon), where  $n$  is the atomic number density. For each collision step, the impact parameter is sampled by randomly choosing a point within a disk of area  $\sigma_{\text{geo}} = n^{-2/3}$ . The scattering angle and hence elastic energy transfer is determined by a Molière interatomic potential. Inelastic interactions were modeled by sampling the measured Ar-Ar ionization and excitation cross sections for each collision with probabilities  $p_{\text{ion}} = \sigma_{\text{ion}}/\sigma_{\text{geo}}$  and  $p_{\text{exc}} = \sigma_{\text{exc}}/\sigma_{\text{geo}}$ . Figure 2 depicts the inelastic argon cross sections compiled by Phelps [10]. The inelastic energy losses were accounted for in the energy budget of each cascade as follows. For collision energies  $< 1$  keV, ionization is primarily produced via the creation of the auto-ionizing state ( $1s^2 2s^2 2p^6 3s^1 3p^6 4s^1$ ) with excitation energy  $\sim 25$  eV, leading to the subsequent emission of an electron of energy  $\sim 9$  eV [11]. The exiting  $\text{Ar}^+$  projectile neutralizes quickly by charge exchange ( $\sigma_{\text{cx}} \sim 10^{-15}$  cm<sup>2</sup>), with its energy reduced by the ionization potential of argon ( $I_p(\text{Ar}) \sim 15.6$  eV). The total inelastic energy loss per ionization of  $\sim 41$  eV is subtracted from the projectile energy. Excited  $\text{Ar}^*$  atoms are assumed to be created in state ( $1s^2 2s^2 2p^6 3s^2 3p^5 4s^1$ ) with energy  $\sim 12$  eV. The primary projectile and all energetic secondary particles produced in the cascade are followed till their energies drop below the inelastic reaction threshold ( $\sim 25$  eV in the laboratory frame).

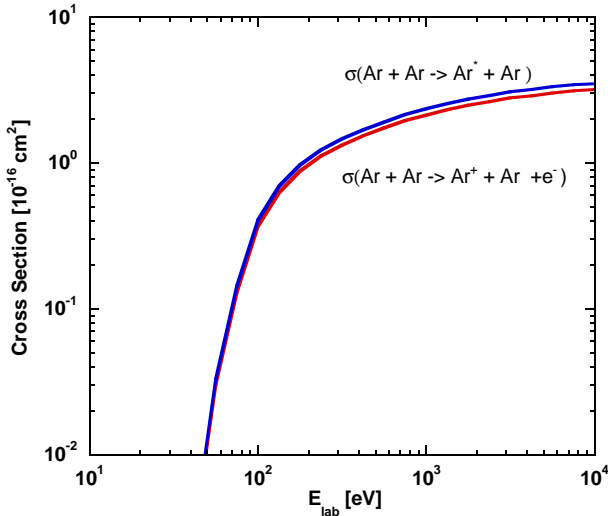


Fig. 2: Excitation and ionization cross sections for Ar + Ar collisions.

The code allowed us to calculate the energy-dependent ionization and excitation yields, and thus determine the Ar quench factor (shown in Figure 3), defined here as

$$Q(E) \equiv \frac{[N_{\text{ion}} + N_{\text{exc}}]_{\text{nucl}}}{[N_{\text{ion}} + N_{\text{exc}}]_{\text{elec}}} \approx \frac{[N_{\text{ion}} + N_{\text{exc}}]_{\text{nucl}}}{1.21(E/W)},$$

where  $N_{\text{ion}}$  and  $N_{\text{exc}}$  are the energy-dependent average ionization and excitation numbers, and  $W$  is the average electronic energy required to produce an electron-ion pair [12].

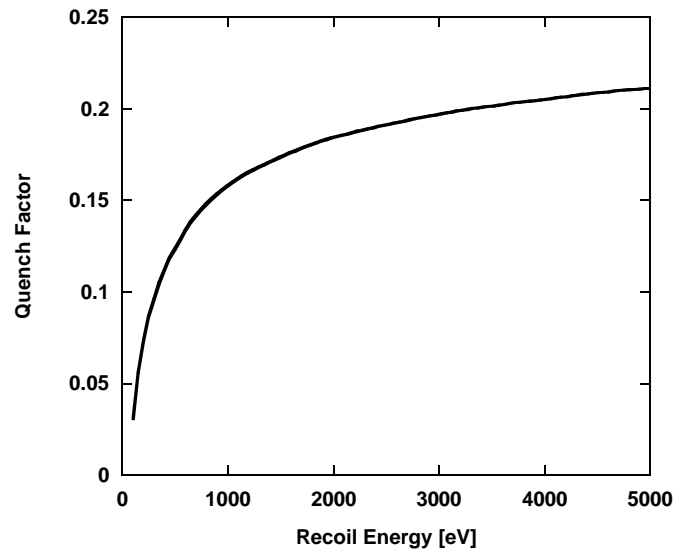


Fig. 3: Quench factor of argon, defined as the ratio of nuclear to electron recoil ionization & excitation yield. A  $W$  value of 26 eV is used. Atomic argon ionization and excitation contribute equally to  $Q$  due to their nearly identical cross sections.

We obtained the reactor neutrino ionization spectrum, depicted in Figure 4, by convolving the ionization efficiency with the recoil spectrum. About 29 % of all recoils produce at least a single electron-ion pair. In addition, a similar number of  $\text{Ar}^*$  is created with an identical number spectrum. Some of the excitation can be converted into ionization via doping with xenon. Since the  $\text{Ar}^*$  exciton energy exceeds the ionization potential of xenon in liquid argon ( $I_p(\text{Xe}) \sim 10.6$  eV), the secondary ionization process ( $\text{Ar}^* + \text{Xe} \rightarrow \text{Ar} + \text{Xe}^+ + e^-$ ) is energetically allowed. Experimentally [12], the probability for this Penning mechanism to occur is

### III. DETECTOR SCHEME

$$p_{\text{Penning}} = \frac{1.44 f_{\text{Xe}} [\%]}{1 + 1.44 f_{\text{Xe}} [\%]} ,$$

where  $f_{\text{Xe}}$  is the xenon concentration in liquid argon. The number of free electrons created in argon is consequently enhanced to

$$N_e = N_{\text{ion}} + p_{\text{Penning}} N_{\text{exc}} .$$

Table 1 summarizes the expected recoil and ionization rates.

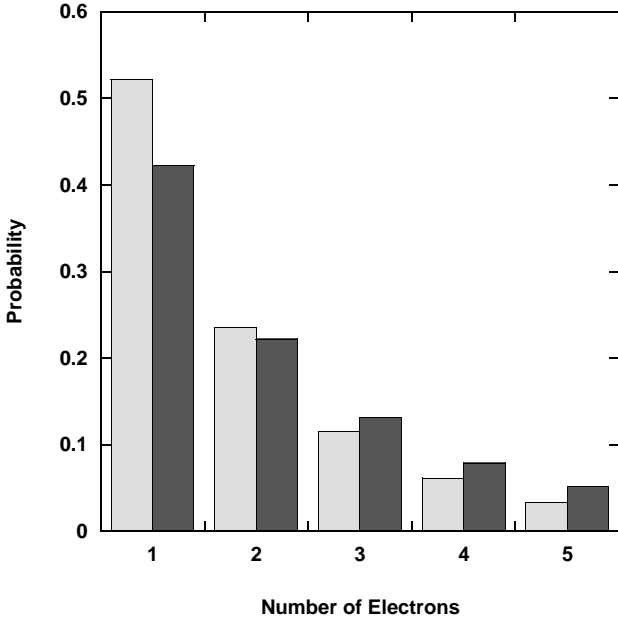


Fig. 4: Ionization number spectrum arising from reactor neutrinos. The light-shaded bins represent the spectrum for pure argon, the dark-shaded bins are for argon doped with ~ 1% xenon.

Table 1: Signal parameters for a reactor neutrino flux of  $6 \times 10^{12} \text{ cm}^{-2} \text{ s}^{-1}$  from a typical 3 GWt core

Average argon recoil energy	234 eV
Number of recoils per day per 10 kg of argon	560
Fraction of ionizing recoils in pure argon	29 %
Fraction of ionizing recoils with 1% xenon doping	36 %

Emission detectors house two phases (liquid-gas or liquid-solid) of a noble element in a single cell [13]. They may combine a large detector mass with a low detection threshold, and are ideally suited for measuring rare events in the keV range. The primary ionization event most likely takes place in the condensed phase of the detector, where free electrons are produced. An applied electric field causes the electrons to drift towards the phase boundary, cross into the gas, and amplify the charge signal via electroluminescence (proportional scintillation). Geminate recombination and capture on electronegative  $\text{O}_2$  impurities may lead to electron loss. The rate of the former is proportional to the product of the positive and negative charge density and thus small for weak ionization events. The latter process can be made negligible by keeping the transfer time smaller than the free electron lifetime. Bakale et al. [14] measured an attachment lifetime of

$$t_a \approx \frac{10^{-11}}{[\text{O}_2]/[\text{Ar}]} \text{ s} ,$$

and lifetimes of a few ms are routinely achieved using commercially available purification systems.

The electron transfer time (between primary event time till detection in the gas region) is usually dominated by the drift time  $\tau_d$  (in the liquid), and the phase boundary crossing time  $\tau_x$ . The electron drift velocity in liquid argon is electric field dependent. For the range  $10^2 \text{ V/cm} < \epsilon < 10^3 \text{ V/cm}$ , the drift time  $\tau_d$  over a distance  $L_d$  (in cm) is approximately given by [15]

$$t_d \approx 10^{-5} L_d \left( \frac{\epsilon}{300 \text{ V/cm}} \right)^{-0.64} \text{ s} .$$

The electronic potential barrier height of the liquid-gas interface in argon is ~ 0.2 V, and the electrons are transferred into the gas by field-assisted thermionic emission. Borghesani et al. [16] determined a crossing time of

$$t_x \approx \frac{0.1}{\epsilon} e^{-0.06\epsilon^{1/2}} \text{ s} ,$$

where  $\epsilon$  has units of V/cm.

Once in the gas phase, the electrons traverse an electroluminescence gap defined by two parallel grids with an applied potential of a few kV. Inelastic collisions create  $\text{Ar}_2^*$  molecules which decay radiatively, emitting UV photons of energy ~ 10 eV. Both singlet and triplet states are created, with lifetimes of 4 ns and 3  $\mu\text{s}$  respectively [17]. Dias et al. [18]

have extensively modeled the scintillation efficiency as a function of the reduced field  $e/n$ . The light conversion efficiency rises from the threshold value  $(e/n)_c = 3 \times 10^{-17} \text{ Vcm}^2$  roughly linearly to  $\sim 50\%$  at  $(e/n) = 7 \times 10^{-17} \text{ Vcm}^2$ . Gain values of a few hundred photons per electron with a cm scale gap are typical. Lastly the UV light needs to be collected with high efficiency to enable detection of single electrons. Both large-area, UV-sensitive phototubes and windowless avalanche diodes are attractive options. Figure 5 shows a schematic of the detector we envisage for this experiment.

#### IV. CALIBRATION

The detector could be calibrated for example by fast neutron elastic scattering [5] or by thermal neutron capture [3,6]. The latter is well suited for producing sub-keV recoil energies in argon. The  $^{40}\text{Ar}(n,\gamma)^{41}\text{Ar}$  reaction has a  $Q = 6.098 \text{ MeV}$ , which is released into two characteristic gamma rays ( $E_1 = 5.58 \text{ MeV}$ ,  $E_2 = 0.516 \text{ MeV}$ ) with a branching ratio of  $\sim 10\%$ . The first gamma gives a recoil  $E_r = \frac{1}{2} E_1^2/M_{\text{Ar}} = 415 \text{ eV}$ , while the second one could be used for tagging the recoil.

#### V. BACKGROUNDS

Low energy (few electrons) events may be caused by (1) small angle Compton recoils from internal and external gamma radioactivity, and (2) nuclear recoils arising from elastic neutron scattering. Backgrounds due to external gamma/neutron activity can be reduced by lead/polyethylene shielding and operating the detector at a shallow underground site near the reactor. Figure 6 shows the estimated background rates in a bare detector and for a dual-shield configuration. The background issues are similar to those encountered in WIMP detector, although a reactor neutrino detector would have substantially higher signal rates, thus rendering the internal radiopurity and shielding requirements less problematic. Because only the ionization signal is measured, there is no way of discriminating between nuclear and electronic recoils.

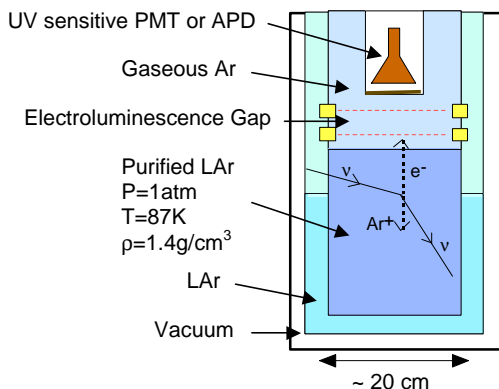


Fig. 5: Schematic of proposed detector.

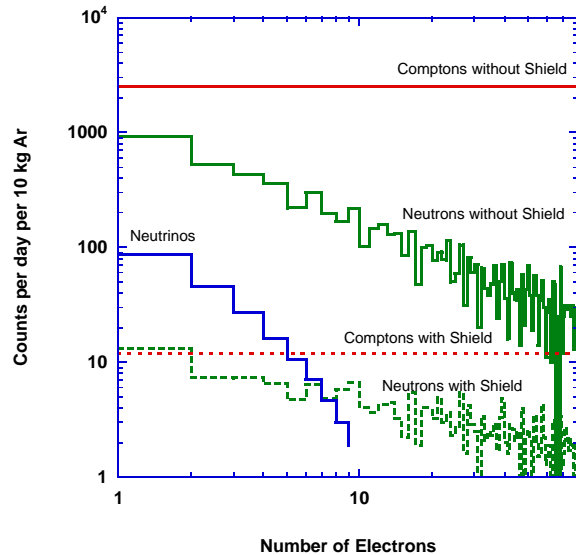


Fig. 6: Monte Carlo simulation of gamma and neutron induced detector backgrounds. Characteristic gammas ( $E > 50 \text{ keV}$ ) were sourced isotropically within a 20 cm thick concrete wall surrounding the argon detector. The concrete had U/Th/K activities of 104/47/533  $\text{mBq/cm}^3$  respectively. With regard to neutrons, an isotropic source with flux  $\sim 10^5 \text{ m}^{-2}\text{s}^{-1}$  (detector site depth = 20 mwe), and a 1/E spectrum from thermal energies up to 20 MeV was used in the simulation. A reduction of the backgrounds by  $\sim 100$  is achieved with a layered shield of 2 cm of lead (inner) and 10 cm of borated polyethylene (outer).

#### VI. ACKNOWLEDGMENT

This work was performed under the auspices of the U.S. Department of Energy by University of California, Lawrence Livermore National Laboratory under Contract W-7405-Eng-48. We thank A. Bolozdynya for illuminating discussions.

#### VII. REFERENCES

- [1] A. Drukier and L. Stodolsky, "Principles and applications of a neutral-current detector for neutrino physics and astronomy" *Phys. Rev. D* 30, pp. 2295-2309, 1984.
- [2] B. Cabrera, L. M. Krauss, and F. Wilczek, "Bolometric detection of neutrinos" *Phys. Rev. Lett.* 55, pp. 25-28, 1985.
- [3] P. S. Barbeau, J. I. Collar, J. Miyamoto, and I. Shipsey, "Toward coherent neutrino detection using low-background micropattern gas detector" *IEEE Trans. Nucl. Sci.*, vol. 50, no. 5, pp. 1285-1289, Oct. 2003.
- [4] A. S. Starostin and A. G. Beda, "Germanium detector with internal amplification for investigating rare processes" *Phys. Atom. Nucl.* 63, pp. 1297-1300, 2000.
- [5] G. Gerbier et al., "Measurement of the ionization of slow silicon nuclei in silicon for the calibration of a silicon dark-matter detector" *Phys. Rev. D* 42, pp. 3211-3214, 1990.

- [6] K. W. Jones and H. W. Kraner, "Energy lost to ionization by 254-eV  $^{73}\text{Ge}$  atoms stopping in Ge" *Phys. Rev. A* 11, pp. 1347-1353, 1975.
- [7] P. Vogel and J. Engel, "Neutrino electromagnetic form factors" *Phys. Rev. D* 39, pp. 3378-3383, 1989.
- [8] G. Zacek et al., "Neutrino-oscillation experiments at the Gösgen nuclear power reactor" *Phys. Rev. D* 34, pp. 2621-2636, 1986.
- [9] J. P. Biersack and L. G. Haggmark, "A Monte Carlo computer program for the transport of energetic ions in amorphous targets" *Nucl. Instr. and Meth. In Phys. Res.* 174, pp. 257-320, 1980.
- [10] A. V. Phelps "Cross sections and swarm coefficients for nitrogen ions and neutrals in  $\text{N}_2$  and argon ions and neutrals in Ar for energies from 0.1 eV to 10 keV" *J. Phys. Chem. Ref. Data* 20(3), pp. 557-573, 1991.
- [11] G. Gerber, R. Morgenstern, and A. Niehaus, "Ionization processes in slow collisions of heavy particles II. Symmetrical systems of the rare gases He, Ne, Ar, Kr" *J. Phys. B: Atom. Molec. Phys.* 6, pp. 493-510, 1973.
- [12] S. Kubota et al., "Evidence of the existence of exciton states in liquid argon and exciton-enhanced ionization from xenon doping" *Phys. Rev. B* 13, pp. 1649-1653, 1976.
- [13] A. Bolozdynya, "Two-phase emission detectors and their applications" *Nucl. Instr. and Meth. In Phys. Res.* A422, pp. 314-320, 1999.
- [14] G. Bakale, U. Sowada, and W. F. Schmidt, "Effect of an electric field on electron attachment in  $\text{SF}_6$ ,  $\text{N}_2\text{O}$ ,  $\text{O}_2$  in liquid argon and xenon" *J. Phys. Chem.* 80, pp. 2556-2559, 1976.
- [15] T. Doke "Fundamental properties of liquid argon, krypton, and xenon as radiation detector material" *Portugal Phys.* 12, pp.9-48, 1981.
- [16] A. F. Borghesani et al., "Electron transmission through the Ar liquid-vapor interface" *Phys. Lett. A* 149, pp. 481-484, 1990.
- [17] N. Schwentner, E.-E. Koch, and J. Jortner, *Electronic excitations in condensed rare gases*. Berlin, Springer Verlag, 1985.
- [18] T. H. V. T. Dias, A. D. Stauffer, and C. A. N. Conde, "A unidimensional Monte Carlo simulation of electron drift velocities and electroluminescence in argon, krypton, and xenon" *J. Phys. D: Appl. Phys.* 19, pp. 527-545, 1986.